



Published in final edited form as:

*Biomacromolecules*. 2012 November 12; 13(11): 3850–3857. doi:10.1021/bm3013023.

## Intravenous Hemostatic Nanoparticles Increase Survival Following Blunt Trauma Injury

Andrew J. Shoffstall<sup>1</sup>, Kristyn T. Atkins<sup>1</sup>, Rebecca E. Groynom<sup>1</sup>, Matthew E. Varley<sup>1</sup>, Lydia M. Everhart<sup>1</sup>, Margaret M. Lashof-Sullivan<sup>1</sup>, Blaine Martyn-Dow<sup>1</sup>, Robert S. Butler<sup>2</sup>, Jeffrey S. Ustin<sup>3</sup>, and Erin B. Lavik<sup>1</sup>

<sup>1</sup>Department of Biomedical Engineering, Case Western Reserve University, Cleveland, OH 44106

<sup>2</sup>Department of General Surgery, Cleveland Clinic, Cleveland, OH 44195

<sup>3</sup>Department of Quantitative Health Sciences, Cleveland Clinic, Cleveland, OH 44195

### Abstract

Trauma is the leading cause of death for people ages 1-44, with blood loss comprising 60-70% of mortality in the absence of lethal CNS or cardiac injury. Immediate intervention is critical to improving chances of survival. While there are several products to control bleeding for external and compressible wounds including pressure dressings, tourniquets or topical materials (e.g. QuikClot, HemCon), there are no products that can be administered in the field for internal bleeding. There is a tremendous unmet need for a hemostatic agent to address internal bleeding in the field.

We have developed hemostatic nanoparticles (GRGDS-NPs) that reduce bleeding times by ~50% in a rat femoral artery injury model. Here, we investigated their impact on survival following administration in a lethal liver resection injury in rats. Administration of these hemostatic nanoparticles reduced blood loss following the liver injury and dramatically and significantly increased 1-hour survival from 40 and 47% in controls (inactive nanoparticles and saline, respectively) to 80%. Furthermore, we saw no complications following administration of these nanoparticles. We further characterized the nanoparticles' effect on clotting time (CT) and maximum clot firmness (MCF) using rotational thromboelastometry (ROTEM), a clinical measurement of whole-blood coagulation. Clotting time is significantly reduced, with no change in MCF. Administration of these hemostatic nanoparticles after massive trauma may help staunch bleeding and improve survival in the critical window following injury, and this could fundamentally change trauma care.

### Keywords

hemostasis; survival; clotting; platelets; bleeding

---

Trauma is the leading cause of death for individuals between ages 1-44.<sup>1</sup> More than one-third of patients die before reaching the hospital.<sup>1</sup> In military trauma, outcomes are even worse.<sup>2</sup> Injuries are often more severe and can have the additional complication of a prolonged prehospital phase, defined as the time between injury and admission to the hospital.<sup>2, 3</sup> Hemorrhage accounts for 50% of penetrating battlefield trauma mortality, and 80% of these deaths are secondary to injury in the torso, where conventional methods for hemostasis, such as pressure dressings, tourniquets, QuikClot, or HemCon are impossible

(noncompressible injuries).<sup>2, 4-6</sup> The way Clifford<sup>5</sup> poses the challenge is that while civilian blunt trauma patients may have a “golden hour”, military personnel with penetrating trauma may only have a “platinum 5 minutes”, during which, catastrophic hemorrhage may occur. This places a large emphasis on the first-response medics to stabilize patients prior to transportation to a hospital. For civilian and non-civilian application, there is a tremendous unmet need for a field-administrable hemostatic agent to address internal hemorrhage.<sup>3</sup>

There is a dearth of tools to address internal bleeding. Methods that have been pursued include blood and blood product transfusions, and treatment with clotting factors such as recombinant factor VIIa (RFVIIa).<sup>7</sup> Resuscitative strategies with blood components such as fibrinogen or platelets are limited by their necessity for donor sources, immunocompatibility, need for refrigeration and risk of loss of activity during storage or preservation methods.<sup>7</sup> These complications limit their use to hospital settings. The administration of recombinant factor VIIa intravenously to reduce bleeding after acute trauma has been a topic of debate.<sup>5, 8-10</sup> Several studies have shown that perioperative administration of RFVIIa reduces the volume of blood transfusion. However, it is unclear whether the benefit is large enough to have any associated effect on mortality after hemorrhagic trauma.<sup>11, 12</sup> Its potential use in the prehospital phase is further diminished due to its high cost, potential for adverse effects, and necessity to be stored at 2-8 °C.<sup>8, 13</sup>

Intravenous administration of hemostatic nanoparticles that target activated platelets have been investigated by a number of groups with some promise and a range of challenges.<sup>14-16</sup> RGD conjugated red blood cells (RBCs) called thromboerythrocytes showed promise *in vitro* but did not significantly reduce prolonged bleeding times in thrombocytopenic primates.<sup>14, 17</sup> Furthermore, the use of allogenic RBCs may produce an immune response in the recipient that further impedes clinical translation.<sup>18</sup> Fibrinogen-coated albumin microparticles (3.5-4.5 μm diameter), “Synthocytes,”<sup>19</sup> and liposomes (220 nm diameter) carrying the fibrinogen γ chain dodecapeptide (HHLGGAKQAGDV)<sup>20, 21</sup> showed success in bleeding models in thrombocytopenic rabbits. However, Synthocytes were ineffective in treating bleeding in normal rabbits<sup>19</sup> and may be hindered by their large size; Merkel et al. has shown that particles, especially those that are large and not mechanically compliant, are prone to aggregation in the lungs, which may increase the propensity for pulmonary complications.<sup>22, 23</sup> The liposomes from Okamura et al.<sup>20, 21</sup> do not appear to have yet been studied in non-thrombocytopenic animals.

From this work, several things are clear. First, large particles and those including potentially immunogenic materials (i.e. biologically derived materials) carry additional and possibly unnecessary risks. Second, what works *in vitro* may not translate to *in vivo* conditions, or to the general (non-thrombocytopenic) trauma population. Because the coagulation system is so complex, multiple bleeding models (and species) with functionally-directed outcomes, in concert with *in vitro* studies, are required to fully evaluate a potential therapy, as has been recognized by the FDA in a set of published guidelines for platelet substitutes.<sup>24</sup> Prothrombotic potential, immunogenicity, and toxicity due to additives are among the safety criteria, and efficacy criteria is based on a battery of *in vivo* and *in vitro* tests.

We have developed novel hemostatic nanoparticles (GRGDS-NPs) that can be administered intravenously to reduce bleeding times by ~ 50% in a model of rat femoral artery injury, performing better than saline or RFVIIa controls.<sup>25</sup> These nanoparticles are made of biodegradable polymers, reducing the risk of long-term immunological and inflammatory reactions. The salient features of these nanoparticles include a 400 nm core made of biodegradable block copolymer of poly(lactic-co-glycolic acid) (PLGA) and poly-ε-L-lysine(PLL) with poly(ethylene glycol) (PEG) arms terminated with arginine-glycine-aspartic acid (**GRGDS**)-based targeting ligands (Figure 1a). GRADSP ligands are used as a

scrambled peptide to control for nonspecific actions of the particles (Scrambled-NPs). For research purposes, the nanoparticles have been loaded with coumarin-6, a fluorescent dye that allows us to track their Biodistribution.<sup>25</sup>

In this study, we investigated the impact of intravenous delivery of the GRGDS-NPs on blood loss and survival in a clinically relevant model of blunt trauma. We sought to evaluate our treatment *in vivo* and *in vitro* to help elucidate efficacy and mechanism. We investigated the nanoparticles in a lethal liver injury model to determine 1) whether the nanoparticles had an effect in a complex solid organ injury, 2) if that effect produced any functional impact on blood loss and mortality outcomes, and 3) to investigate the effects of the nanoparticles on clotting time and clot firmness parameters using rotational thromboelastometry (ROTEM), to better understand the mechanism by which the nanoparticles augment hemostasis. The data from these studies is a critical step in determining the clinical potential of these particles and gaining insight into nanomedicine more broadly.

## MATERIALS AND METHODS

### Materials

PLGA (Resomer 503H) was purchased from Evonik Industries. Poly-L-lysine and PEG (~4600 Da MW) were purchased from Sigma Aldrich. All reagents were ACS grade and were purchased from Fisher Scientific.

### Particle synthesis

A PLGA-PLL-PEG triblock polymer was synthesized using stepwise conjugation reactions, starting with PLGA (Resomer 503H) and poly( $\epsilon$ -cbz-L-lysine) (PLL-cbz) PLL with carbobenzoxy-protected side amine side groups (Sigma P4510) as previously described.<sup>25</sup> This conjugation reaction was confirmed using UV-Vis to check for a signature triple peak corresponding to the cbz groups. After deprotecting the PLGA-PLL-cbz with HBr, the free amines on the PLL-NH<sub>3</sub> were reacted with CDI-activated PEG in a 5:1 molar excess.<sup>27</sup> The conjugated triblock copolymer PLGA-PLL-PEG (with CDI activated PEG endgroups) was dissolved to a concentration of 20 mg/ml in acetonitrile containing coumarin-6 (C6), a fluorescent dye is used to track the nanoparticles after injection (loaded at 1% w/w). This dye has been shown previously to release less than 0.5% of the initial loading by 24 h and less than 1.5% by 7 days.<sup>25</sup> This solution was added dropwise to a volume of stirring PBS, twice that of the acetonitrile.<sup>28</sup> Precipitated nanoparticles form as the water-miscible solvent is displaced. The nanoparticles were then conjugated with GRGDS or the conservatively substituted GRADSP peptide and stir-hardened for 3 hours in a single step. Nanoparticles were then collected using the coacervate precipitation method described below.

### Coacervate precipitation and resuspension

The method for nanoparticle collection was adapted from D'Addio et al.<sup>29</sup> One mass equivalent of dry poly(acrylic acid) (pAA) (Sigma, MW = 1,800) was added to the stirring particle suspension. 1% w/v pAA was then added to the stirring suspension until flocculation occurred, approximately 10 ml. After 5 minutes, the flocculated nanoparticles were collected by centrifugation and rinsed 3 times. Nanoparticles were resuspended to approximately 10 mg/ml with deionized water, snap-frozen in liquid nitrogen and lyophilized for 3 days. Nanoparticles were resuspended to a concentration of 20 mg/ml in 1x PBS and briefly sonicated (VCX-130, Sonics & Materials, Inc.).

### Characterization

Nanoparticles were characterized for size distribution, size polydispersity and zeta potential (in 1 mM KCl buffer) using dynamic light scattering (90Plus, Brookhaven Instruments

Corporation) and scanning electron microscopy (Hitachi S4500). DLS data was represented as the effective diameter as calculated by the 90Plus software. SEM images were analyzed in ImageJ software. Successful conjugation of PLL, PEG and peptide ligands was confirmed using UV-spectroscopy, <sup>1</sup>H-NMR and amino acid analysis HPLC (BioRad, Varian and Shimadzu respectively). <sup>1</sup>H-NMR is performed with chloroform for analyzing the triblock structure and deuterated water to verify the PEG coronal shell.<sup>30</sup> Amino acid analysis was performed by W.M. Keck Foundation Biotechnology Resource Laboratory (New Haven, CT).

### ***In vitro* coagulation assay (ROTEM)**

Coagulation assays, using Sprague Dawley rat blood, were performed using the ROTEM's NATEM test in the presence of either saline, GRGDS-NPs, or scrambled GRADSP-NPs. The blood collection method (cardiac puncture) was rigidly followed to minimize variability in the highly sensitive NATEM test. A 5 ml syringe is loaded with 0.5 ml of 3.8% disodium citrate prepared in 1x PBS. Rats were anesthetized with a ketamine:xylazine rodent cocktail (90:10 mg/kg, i.p.). 4.5 ml of blood is collected to mix with the anticoagulant solution at a 1:9 ratio (soln: blood). For a given run, the cup of blood consisted of: 300  $\mu$ l citrated blood, 20  $\mu$ l starTEM reagent (0.2 mM calcium chloride), 20  $\mu$ l nanoparticles (1.25 or 2.5 mg/ml), totaling a 340  $\mu$ l sample. To account for time dependency on coagulation tests, a block of 4 NATEM tests were run simultaneously on a single ~1.2 cc aliquot of blood, where saline was always included as one of the four tests. The raw data was analyzed using a generalized linear model, with run time as blocks and with Tukey comparisons between groups. The main outcomes we considered include the standard ROTEM parameters clotting time (CT), clot formation time (CFT), the sum of the two (CT+CFT), and maximum clot firmness (MCF). CT is defined as the time from the start of the assay until the initial clotting is detected (thickness = 2mm). CFT is defined as the time between the initial clot (thickness = 2mm) until a clot thickness of 20 mm is detected. MCF is defined as the maximum thickness (in mm) that a clot reaches during the duration of the test.

### ***In vivo* liver injury model**

In order to assess the efficacy of the nanoparticles to augment survival in a lethal injury model, a liver injury model was adapted from Ryan et al.<sup>31</sup> and Holcomb et al.<sup>32</sup> and is described below. The injury model was approved and undertaken according to the guidelines set by Case Western Reserve University's institutional animal care and use committee. The main outcomes recorded for this study include survival at 1 hour and blood loss as measured with pre-weighed gauze.

### **Surgical procedure**

Sprague Dawley rats (225-275 g, Charles River) were anesthetized with intraperitoneal ketamine:xylazine (90:10 mg/kg, respectively). After 10 minutes, they were shaved and placed in a supine position on a heatpad. The abdomen was accessed and the medial lobe of the liver was marked with an arch radius 1.3 cm from the suprahepatic vena cava using a handheld cautery device. Once marked, the tail vein was exposed, and catheterized with a saline-flushed 24G x 3/4" Excel Safelet Catheter. The medial liver lobe was then resected along the marked lines, the abdomen was closed with wound clips, and 0.5 cc bolus treatment solution was immediately administered followed by 0.2 cc saline flush to clear the catheter dead-volume.

The rats were allowed to bleed for 1 hour or until death, as confirmed by lack of both breathing and a palpable heartbeat. Before measuring blood loss, all rats were injected with a lethal dose of sodium pentobarbital (i.v.). The abdomen was then reopened and blood collected with pre-weighed gauze. The clot adherent to the liver was collected last as this

usually caused additional bleeding to occur. The resected liver was weighed and fixed in 10% buffered formalin solution. Remaining liver, kidney, spleen, lungs and adherent clot were harvested and similarly preserved in 10% buffered formalin.

### Procedure and statistics

Treatments included no injection (n=3), saline (n=17), scrambled-NPs (n=15), and hemostatic GRGDS-NPs (n=20). Particle treatments were resuspended to 20 mg/ml in PBS. The surgeon was blinded to the treatments and all blood loss measurements and death were independently recorded by a second person also blinded to the treatment. The no injection group (n=3) was included as a reference, but was not included in the statistics. ANOVA with Tukey comparisons was used to analyze blood loss data (Minitab). Survival was analyzed with a binomial logistic regression with chi-squared tests between odds-ratios (SAS). A power analysis based on preliminary studies suggested an n=15 per group for significance for survival data ( $\alpha = 0.05$ ,  $\beta = 0.2$ , odds ratio = 3).

### Biodistribution

Liver, kidney, spleen, lung and adherent clots were harvested and lyophilized for the biodistribution assay. The dry weight of the whole organ was recorded and 100-200 mg of dry tissue was homogenized (Precellys 24) and incubated overnight in acetonitrile at 37 °C. This dissolved any nanoparticles present in the tissue and left the C6 in the organic solvent solution. Tubes were then centrifuged at 15,000 g for 10 minutes to remove solid matter and supernatant was tested on the HPLC. Mobile phase was 80% acetonitrile, and 20% aqueous (8% acetic acid). Stationary phase was a Waters Symmetry C18 Column, 100Å, 5 Um, 3.9 mm X 150 mm with fluorescence detection (450/490 nm ex/em). Based on the known C6 loading and injection volume of particles, data is represented as percent (%) of particles injected.

### Imaging injury surface and adherent clots

Resected portions of the liver were rinsed and placed directly on a high-resolution (1200 dpi) flatbed scanner (Cannon CanoScan LiDE 700F) to image the surface of the injury. Adherent clots, still attached to livers were fixed in 10% formalin, soaked overnight in sucrose, frozen and cryosectioned to 20-micron thickness. Sections were then stained with VectaShield DAPI to stain hepatocyte nuclei and imaged with an inverted fluorescence microscope (Zeiss Axio Observer.Z1). Several clots per group were fixed in 10% formalin, and dehydrated in serial steps with ethanol to prepare them for imaging with a scanning electron microscope (SEM). These were then dried overnight in anhydrous hexamethyldisilazane and sputter coated. Samples were mounted and imaged with a Hitachi S4500 field emission SEM at 5kx magnification.

## RESULTS

### Particle synthesis and characterization

The PLGA-PLL-PEG triblock polymer is synthesized using stepwise conjugation reactions, starting with PLGA (Resomer 503H) and poly( $\epsilon$ -cbz-L-lysine) PLL with carbobenzoxy-protected side amine side groups following Bertram et al.<sup>25, 26, 33</sup> Conjugation efficiency for this step is approximately ~30-40% molar ratio PLL:PLGA, as determined by UV-vis. After deprotection of side groups, the free amines on the PLL are reacted with CDI-activated PEG. This PEG creates a hydrophilic shell around the nanoparticles that allow them to have a longer residence time in blood circulation<sup>30</sup> (Figure 1a). <sup>1</sup>H-NMR in deuterated chloroform and deuterated water is performed to verify the expected surface-pegylated structure (Figure 1c). Peaks a, b, and d confirm the composition of PLGA (50:50), and peak

c confirms the presence of PEG. From this spectrum, percent pegylation is calculated to be 1:10 (PEG:PLGA) molar ratio. In deuterated water, the PEG peak becomes much larger in relation to the other peaks and confirms the PEG-coronal structure of the nanoparticles in an aqueous environment. This is further verified by a neutral zeta potential result when making nanoparticles consisting of the PLGA-PLL-PEG triblock polymer, suggesting the positively charged PLL is shielded by PEG. However, once incorporated, the surface-conjugated peptides do impart a slightly negative charge:  $-27.84 \text{ mV} \pm 2.76 \text{ mV}$  for the GRGDS-NPs and  $-13.47 \text{ mV} \pm 3.64 \text{ mV}$  for the scrambled-NPs. The size and distribution of the nanoparticles cores (by SEM) and in the aqueous environment (by DLS) is homogeneously distributed around 400 nm and 420 nm respectively (Table 1). The increase in size from SEM to DLS can be accounted for by the hydration shell, created by the PEG arms. There appears to be a slight increase in size as a result of C6 loading (approximately 5-10%), with no significant change in size depending on the GRGDS or GRADSP peptide conjugated.

### ***In vivo* injury model development**

Following injury of the medial lobe (Figure 1d), rats were administered either saline, scrambled (GRADSP), or hemostatic (GRGDS-conjugated) nanoparticles. Saline is used as the baseline control because the administration of fluids can impact bleeding.<sup>34</sup> Based on our preliminary results, we found that resected liver mass and body mass were correlated with bleeding outcomes, and similar to Holcomb et al.,<sup>32</sup> we chose to strictly adhere to inclusion criteria for rat body mass (225-275 g) and liver resection (0.8-1.2% of body mass) (Figure 2c-d). At the conclusion of the study, we found that body mass was no longer correlated with our bleeding outcomes and we assume our body mass inclusion criteria was a tight enough range to limit its effects on blood loss in our study. However, resected liver mass was still significantly correlated with blood loss ( $p=0.0004$ ), meaning 0.8%-1.2% liver resection (or approximately  $\pm 0.5 \text{ g}$  wet tissue weight), was enough to still significantly affect blood loss outcomes (i.e. a larger resection led to more bleeding, and a smaller resection led to less bleeding). We therefore included resected liver mass as a covariate in our ANOVA analysis to account for its impact. While there is a trend toward reduction in blood loss with the GRGDS-NP group, the impact of treatment on blood loss was still not statistically significant ( $p=0.113$ ).

### **1-Hour survival**

One of the most critical parts of this work was to determine whether administration of the nanoparticles led to improved survival following blunt trauma injury. Administration of the hemostatic, GRGDS nanoparticles significantly improves survival following the lethal liver injury. Specifically, the GRGDS-NPs increases the odds of survival to 80% (Figure 2a-b). This is compared to 47% in the saline group ( $p=0.040$ , odds ratio (OR)=4.5, 95% CI 1.1-19.2) and 40% in the scrambled-NP group ( $p=0.019$ , OR=6, 95% CI 1.3-27.0). Administering the GRGDS-NPs almost doubles the chances of survival from this lethal injury.

### **Blood loss**

We know from our previous work<sup>25</sup> that the GRGDS-NPs reduce bleeding. In this work, we measured blood loss through the weight change in gauze used to absorb the blood in the body cavity at the end of the experiment. This method provides data on blood loss but lacks the fine resolution permitted in the previous study. Measuring total blood loss in this model is complicated by the impact of survival time. The rate of blood loss may be a better indicator of survival for this model, but since the injury model is maintained in the small, closed cavity of rats, blood loss could not be dynamically measured. Nonetheless, we saw a trend in blood loss that correlates with survival with the GRGDS-NPs exhibiting the least

blood loss. This trend towards reduction in blood loss is not statistically significant ( $p=0.0552$ ), but it suggests that the GRGDS-NPs are improving survival through mitigation of bleeding (Figure 2e). There also appears to be a critical threshold around 35% blood volume loss, above which there is rapidly increasing proportion of mortality (Figure 2f).

### Imaging injury surface

To help validate that our GRGDS-NPs are targeting the injury site, and accumulating within the clot, we imaged the injury surface using several modalities including fluorescent microscopy and SEM. Nanoparticles loaded with the fluorescent compound coumarin-6 (C6) are found within the injury surface, integrated with the clot (Figure 3). The injury surface is also characterized using a flatbed scanner to help depict the nature of the injury. From visual observation of the injury during model development, it is apparent that the majority of bleeding occurs through the 2-4 major blood vessels that are transected in the medial lobe injury.

### Biodistribution

For the GRGDS-NPs, 31.1% of the injected dose is found in the clot versus only 6.8% for the scrambled-NP group. Total recovery of the nanoparticles between the clot and organs tested was 53.7% and 29.6% for the GRGDS-NPs and scrambled-NP groups, respectively; the unrecovered proportion is most likely located in the shed blood, not actively participating in the clot, or remaining in plasma circulation. There was a relatively large percentage of nanoparticles found in the lungs for each group, 20.8% and 20.6% (GRGDS and Scrambled, respectively), and a small percentage found in the other organs tested (<2%).

### *In vitro* coagulation model

A dosing study was performed using rotational thromboelastometry (ROTEM), with citrated rat blood. In this assay, a 20  $\mu$ l volume of PBS containing a varying concentration of nanoparticles was added to a 300  $\mu$ l volume of blood immediately before starting the assay. Clotting time (CT) and clot formation time (CFT) were recorded, corresponding to the time it took to form a 2 mm clot size and 20 mm clot size respectively. Here we considered the total time to form a 20 mm clot (CT+CFT). In addition to saline, concentrations of nanoparticles tested included 0.625, 1.25, 2.5, 5.0, and 20 mg/ml for GRGDS and scrambled nanoparticle groups. In all concentrations tested in the scrambled group, the CT+CFT increased and the MCF decreased compared to saline. In GRGDS-NP 1.25 and 2.5 mg/ml concentrations, MCF increased. Similarly, the CT+CFT is decreased in 1.25 mg/ml, and 5.0 mg/ml groups, but was increased otherwise. This is indicative of a clot forming faster and thicker when treated with the nanoparticles at an optimal dose, approximately 73.5-294  $\mu$ g/ml in the blood or a 5.2-20 mg/kg dose for a 250 g male rat, assuming 68.6 ml/kg blood volume.<sup>35</sup>

We then further investigated 1.25 and 2.5 mg/ml concentrations as these had the most favorable effects on clotting parameters. We used a randomized block experimental method, using saline as the control for each test-block. The 2.5 mg/ml GRGDS-NP dose significantly reduced CT+CFT compared to saline controls ( $p=0.0437$ ) and had a trend toward increasing MCF although the difference was not significant ( $n=3$  rats, with triplicate measurements at each treatment-dose level). The 2.5 mg/ml GRGDS-NP dose significantly reduced CT+CFT compared to saline controls ( $p=0.0437$ ) and had a trend toward increasing MCF although not statistically significant. Interestingly, the scrambled-NP groups also appeared to reduce CT+CFT and increase MCF, but the differences were not significantly different from either saline or GRGDS treatments (Figure 5).

## DISCUSSION

### Administration of hemostatic nanoparticles increased 1-hour survival

Early intervention is critical to improve chances of survival following trauma, and we see the effects of early intervention in this work. For all groups tested, there was a window of 20 minutes, after which, the odds of survival improved, as well as a critical blood volume loss of approximately 35% blood volume, below which 95% of rats survived.

Nearly twice as many rats survive one hour with administration of the hemostatic nanoparticles compared to controls. This result is statistically significant and clinically promising. We have seen previously that these hemostatic nanoparticles are stable at room temperature and reduce bleeding in a controlled injury model, but one of the major questions was whether this reduction in blood loss would impact survival in lethal trauma models of bleeding. The liver injury model is one of the most reproducible and comparable in the field.<sup>31, 32, 36</sup> Seeing an almost two fold increase in survival with the GRGDS-NPs confirms that they not only reduce bleeding but do so at a level that impacts survival in the critical prehospital window.

There is a 4.5-fold higher amount of GRGDS-NPs found in the adherent liver clot compared to the scrambled-NP group, with very small quantities of nanoparticles found in the kidney, spleen and uninjured liver, confirming their injury-targeting capability. Nearly 20% of injected nanoparticles have been found in the lungs regardless of the treatment group. While some basal level of nanoparticles in the lungs is expected due to the pulmonary perfusion still present in the organ at the time of collection, previous studies in naïve rats estimate this to account for only 5-10% of the injected dose.<sup>25</sup> These findings may indicate that the nanoparticles could be accumulating in thromboemboli in the lungs, concomitant with the massive hemorrhagic nature of this injury model.<sup>37</sup> However, it is of particular interest to note that survival does not appear to be deleteriously impacted—rather the opposite. It therefore reasons to argue that these thrombi are also present in the saline control, and may be present as microemboli that may not have any clinical presentation.<sup>37, 38</sup> Future studies may be aimed at assessing the risk of particle aggregation in the lungs and determining what functional impacts they may have, for example, by monitoring lung perfusion, tissue oxygenation, or blood gas levels. The ease of intravenous administration of these nanoparticles, coupled with their effective injury-targeting without deleterious functional outcomes bodes well for translation of this therapy to the clinic.

We observed a trend toward reduction in blood loss with the functionalized treatment versus controls. However, the methods for blood collection in trauma models in rats are limited, and the sensitivity is modest at best. Therefore, it is not surprising that we were not able to resolve the differences between the groups in this area to statistical significance. A power analysis to determine the number of animals needed to see differences suggests that an unethically large number of animals would be needed. While this model is not acutely sensitive to differences in blood loss, the trend regarding blood loss correlates well with the survival outcomes, the key point of this study.

One of the questions that plays an important role in the safety and efficacy of a technology like this is the mechanism by which the nanoparticles reduce bleeding. We successfully titrated the optimal whole-blood dosing of the nanoparticles using this *in vitro* model by using rotational thromboelastometry (ROTEM). This confirmed that their effect on clotting times was dose dependent and the optimal dose tested was the 2.5 mg/ml GRGDS-NP group, corresponding to a blood concentration of 147 ug/ml (particle mass/blood volume). Interestingly, the scrambled-NPs have a trend toward an *in vivo* increase in blood loss and a decrease in survival compared to saline. In conjunction with our preliminary ROTEM data



that suggests the scrambled particles may actually decrease MCF at higher concentrations, it is possible that the scrambled-NPs are destabilizing the clot and explain our *in vivo* findings. However, on the other hand, the GRGDS-NPs reduce clotting time and tend to increase clot firmness, so we hypothesize the mechanism for increased survival is more rapid clot formation and increase in clot strength, leading to the reduction in blood loss and increase in survival.

## CONCLUSION

Trauma is the leading cause of death among young people, and blood loss plays a major role in those deaths.<sup>1</sup> We have developed a hemostatic nanoparticle that can be administered easily following injury that reduces bleeding and significantly increases survival following a blunt trauma injury. This is a clinically relevant result as this suggests that this treatment could be used in the field to expand the window of treatment and reduce mortality after hemorrhagic injury. This has the potential to fundamentally impact trauma care and patient outcomes. Further work is indicated to assess the long-term risks associated with hemostatic particle administration and further characterize their efficacy in large animal models where the hemodynamic conditions of flow may have drastic effects on dosing and blood loss outcomes.

## Acknowledgments

The authors would like to acknowledge D. Campbell, L. Wu, and E. Shoffstall for their contributions to this work and a NIH Director's New Innovator Award grant, DP20D007338.

## REFERENCES

- (1). Kauvar DS, Lefering R, Wade CE. *J Trauma*. 2006; 60(6 Suppl):S3–11. [PubMed: 16763478]
- (2). Champion HR, Bellamy RF, Roberts CP, Leppaniemi A. *J Trauma*. 2003; 54(5 Suppl):S13–9. [PubMed: 12768096]
- (3). Holcomb JB, McMullin NR, Pearse L, Caruso J, Wade CE, Oetjen-Gerdes L, Champion HR, Lawnick M, Farr W, Rodriguez S, Butler FK. *Ann Surg*. 2007; 245(6):986–91. [PubMed: 17522526]
- (4). Kauvar DS, Wade CE. *Crit Care*. 2005; 9(Suppl 5):S1–9. [PubMed: 16221313]
- (5). Clifford CC. *Mil Med*. 2004; 169(12 Suppl):8–10. 4. [PubMed: 15651433]
- (6). Morrison JJ, Rasmussen TE. *Surg Clin North Am*. 2012; 92(4):843–58. [PubMed: 22850150]
- (7). Nunez TC, Cotton BA. *Curr Opin Crit Care*. 2009; 15(6):536–41. [PubMed: 19730099]
- (8). Martinowitz U, Zaarur M, Yaron BL, Blumenfeld A, Martonovits G. *Mil Med*. 2004; 169(12 Suppl):16–8. 4. [PubMed: 15651435]
- (9). Patanwala AE. *Am J Health Syst Pharm*. 2008; 65(17):1616–23. [PubMed: 18714107]
- (10). Stein DM, Dutton RP. *Curr Opin Crit Care*. 2004; 10(6):520–8. [PubMed: 15616396]
- (11). Boffard KD, Riou B, Warren B, Choong PI, Rizoli S, Rossaint R, Axelsen M, Kluger Y. *J Trauma*. 2005; 59(1):8–15. discussion 15–8. [PubMed: 16096533]
- (12). Duchesne JC, Mathew KA, Marr AB, Pinsky MR, Barbeau JM, McSwain NE. *Am Surg*. 2008; 74(12):1159–65. [PubMed: 19097529]
- (13). Morse BC, Dente CJ, Hodgman EI, Shaz BH, Nicholas JM, Wyrzykowski AD, Salomone JP, Vercruyse GA, Rozycki GS, Feliciano DV. *Am Surg*. 2011; 77(8):1043–9. [PubMed: 21944521]
- (14). Alving BM, Reid TJ, Fratantoni JC, Finlayson JS. *Transfusion*. 1997; 37(8):866–76. [PubMed: 9280335]
- (15). Blajchman MA. *Vox Sang*. 2000; 78(Suppl 2):183–6. [PubMed: 10938949]
- (16). Blajchman MA. *Transfus Clin Biol*. 2001; 8(3):267–71. [PubMed: 11499975]

- (17). Collier BS, Springer KT, Beer JH, Mohandas N, Scudder LE, Norton KJ, West SM. *J Clin Invest*. 1992; 89(2):546–55. [PubMed: 1737845]
- (18). Vamvakas EC, Blajchman MA. *Blood*. 2009; 113(15):3406–17. [PubMed: 19188662]
- (19). Levi M, Friederich PW, Middleton S, de Groot PG, Wu YP, Harris R, Biemond BJ, Heijnen HF, Levin J, ten Cate JW. *Nat Med*. 1999; 5(1):107–11. [PubMed: 9883848]
- (20). Okamura Y, Maekawa I, Teramura Y, Maruyama H, Handa M, Ikeda Y, Takeoka S. *Bioconjug Chem*. 2005; 16(6):1589–96. [PubMed: 16287259]
- (21). Okamura Y, Eto K, Maruyama H, Handa M, Ikeda Y, Takeoka S. *Nanomedicine*. 2010; 6(2): 391–6. [PubMed: 19699320]
- (22). Merkel TJ, Chen K, Jones SW, Pandya AA, Tian S, Napier ME, Zamboni WE, Desimone JM. *Journal of controlled release : official journal of the Controlled Release Society*. 2012; 162(1): 37–44. [PubMed: 22705460]
- (23). Merkel TJ, Jones SW, Herlihy KP, Kersey FR, Shields AR, Napier M, Luft JC, Wu H, Zamboni WC, Wang AZ, Bear JE, DeSimone JM. *Proceedings of the National Academy of Sciences of the United States of America*. 2011; 108(2):586–91. [PubMed: 21220299]
- (24). Poindexter, B.; Vostal, JG. *Guidance for Industry: For Platelet Testing and Evaluation of Platelet Substitute Products*. FDA. , editor. U.S. Department of Health and Human Services; Bethesda, MD: 1999.
- (25). Bertram JP, Williams CA, Robinson R, Segal SS, Flynn NT, Lavik EB. *Science translational medicine*. 2009; 1(11):11ra22.
- (26). Bertram JP, Jay SM, Hynes SR, Robinson R, Criscione JM, Lavik EB. *Acta biomaterialia*. 2009; 5(8):2860–71. [PubMed: 19433141]
- (27). Hermanson, G. *Bioconjugate Techniques*. 2nd ed. Vol. Vol. 1. Academic Press; San Diego, CA: 2008.
- (28). Cheng J, Teply BA, Sherifi I, Sung J, Luther G, Gu FX, Levy-Nissenbaum E, Radovic-Moreno AF, Langer R, Farokhzad OC. *Biomaterials*. 2007; 28(5):869–76. [PubMed: 17055572]
- (29). D'Addio SM, Kafka C, Akbulut M, Beattie P, Saad W, Herrera M, Kennedy MT, Prud'homme RK. *Mol Pharm*. 7(2):557–64. [PubMed: 20175521]
- (30). Hrkach JS, Peracchia MT, Domb A, Lotan N, Langer R. *Biomaterials*. 1997; 18(1):27–30. [PubMed: 9003893]
- (31). Ryan KL, Cortez DS, Dick EJ Jr, Pusateri AE. *Resuscitation*. 2006; 70(1):133–44. [PubMed: 16757085]
- (32). Holcomb JB, McClain JM, Pusateri AE, Beall D, Macaitis JM, Harris RA, MacPhee MJ, Hess JR. *J Trauma*. 2000; 49(2):246–50. [PubMed: 10963535]
- (33). Lavik EB, Hrkach JS, Lotan N, Nazarov R, Langer R. *J Biomed Mater Res*. 2001; 58(3):291–4. [PubMed: 11319743]
- (34). Matsuoka T, Wisner DH. *J Trauma*. 1996; 41(3):439–45. [PubMed: 8810960]
- (35). Probst RJ, Lim JM, Bird DN, Pole GL, Sato AK, Claybaugh JR. *J Am Assoc Lab Anim Sci*. 2006; 45(2):49–52. [PubMed: 16542044]
- (36). Matsuoka T, Hildreth J, Wisner DH. *J Trauma*. 1995; 39(4):674–80. [PubMed: 7473953]
- (37). Knudson MM, Ikossi DG, Khaw L, Morabito D, Speetzen LS. *Ann Surg*. 2004; 240(3):490–6. discussion 496-8. [PubMed: 15319720]
- (38). Guo G, Kang Y, Li X, Cai ZH, Chen JH, Wang G, Pei GX. *Chin J Traumatol*. 2007; 10(4):237–41. [PubMed: 17651594]

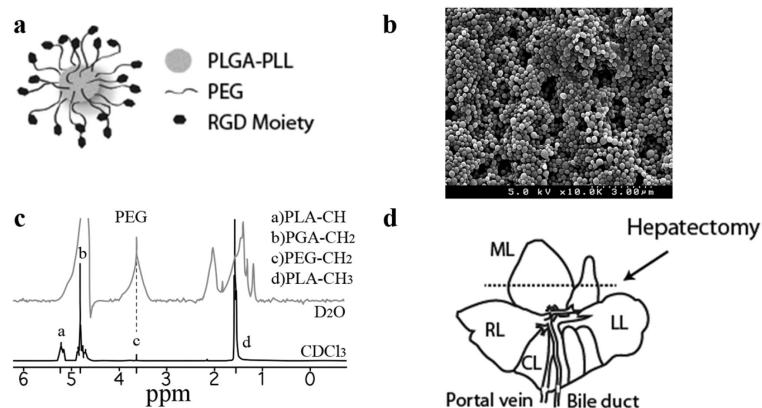


**Figure 1.** Nanoparticle Schematic and Characterization. a) Hemostatic nanoparticles (GRGDS-NPs) consist of PLGA-PLL biodegradable polymer cores, with PEG arms that expose the GRGDS moiety for targeting activated platelets. b) SEM shows nanoparticle size distribution and morphology. c)  $^1\text{H-NMR}$  spectral analysis confirms the pegylation of the co-block-polymer and the PEG-coronal structure of the nanoparticles. Deuterated water (top, gray overlay) and deuterated chloroform (bottom, black overlay). d) These are administered intravenously via the tail vein after a partial hepatectomy in the rat. The medial lobe (ML) is transected in this model. Right (RL), left (LL) and caudate lobes (CL) are labeled for reference.

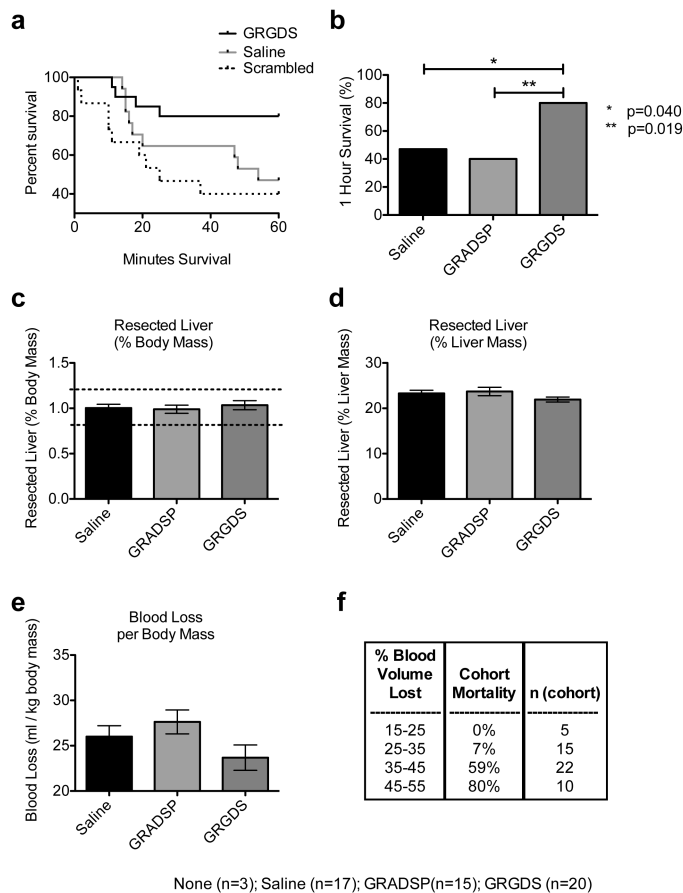


**Figure 2.**

Survival and Blood Loss. a-b) Survival is significantly increased by treatment with the hemostatic GRGDS-functionalized nanoparticles. c-d) The liver mass is tightly controlled in this injury model and is extremely reproducible in size, both in ratio to body mass (1.00%  $\pm$  0.13% S.D.) and in ratio to the remaining liver (22.8%  $\pm$  2.8% S.D.). The dotted lines on the resected liver graph show the inclusion criteria for this study. e) There is a trend toward a reduction in blood loss with the GRGDS-NP group, but is not significantly significant. f) 100% of animals with a blood volume loss less than 32% survive, but rapidly increases above this threshold. Error bars represent SEM.

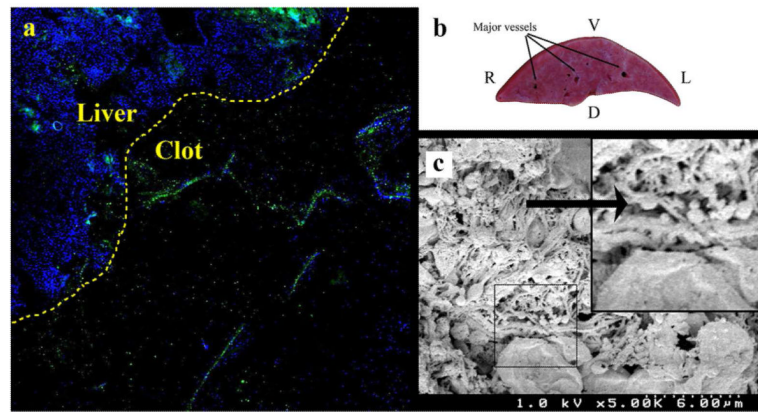


**Figure 3.** Injury Surface Characterization. a) Hemostatic nanoparticles loaded with C6 (green) are found integrated with the adherent clot after it is removed and examined under fluorescent microscopy. b) The majority of bleeding appears to occur from the 2-4 major transected blood vessels in this injury model. c) Scanning electron microscopy is used to verify the presence of the nanoparticles (black arrow) and their integration with the fibrin mesh.

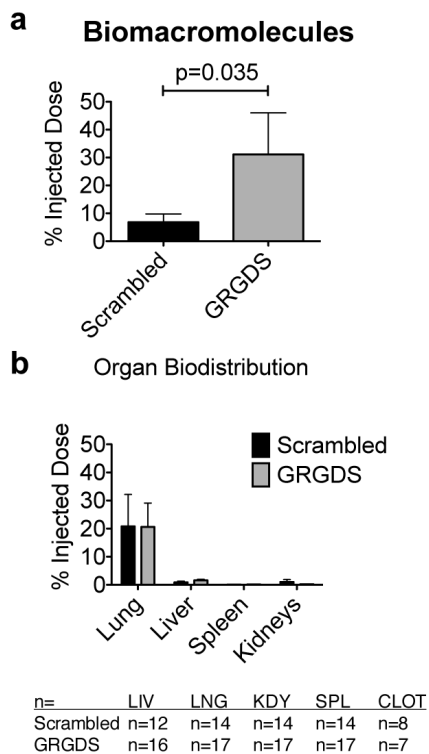


**Figure 4.** Biodistribution. a) 31% of hemostatic GRGDS-NPs locate in the clot, versus 7% for the scrambled-NP control group. Total mean nanoparticle recovery is 53.7% of total injected dose for GRGDS and 29.6% for scrambled. b) The “Liver” group is representative of the particle distribution to the uninjured lower left lobe of the liver. Minimal particle distribution is found in the spleen and kidneys. Approx. 20% is found in the lungs for each formulation. This may be indicative of microemboli in the lung or nanoparticles still in pulmonary circulation.

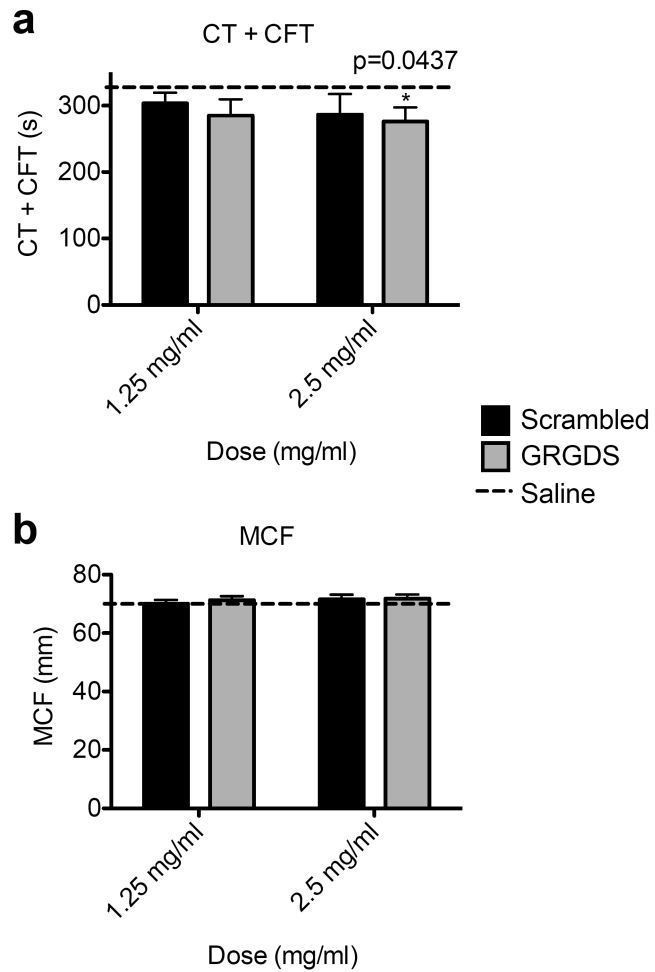


**Figure 5.** In vitro Testing. Outcomes include CT+CFT (a) and MCF (b). The GRGDS group had a lower (faster) clotting time and a higher clot firmness compared to saline. Error bars represent SEM. CT = Clotting Time; CFT = Clot Formation Time; MCF = Maximum Clot Formation; CT+CFT is the sum total of the time it takes from initiation of the experiment until a 20 mm clot is formed.

**Table 1**

Particle characterization: size, polymer composition, and amino acid content.

Nanoparticle Formulation (PLGA-PLL-PEG-X)	SEM - Core dia. [nm] (Mean +/- SD)	DLS - effective dia. [nm] (Mean +/- Polydispersity)	DLS - num. avg. dia. [nm] (Mean +/- SD)	PLL:PLGA (mol:mol)	PEG:PLGA (mol:mol)	Surface Amino Acid X:PEG (mol:mol)
X=GRGDS + C6	391.1 +/- 90.5	419.3 +/- 0.049	431.9 +/- 19.3	0.3:1	0.10:1	0.053:1
X=GRADSP + C6	420.5 +/- 81.7	431.0 +/- 0.005	424.3 +/- 13.4	0.3:1	0.14:1	0.054:1